ERROR BOUNDS OF AREA-AVERAGED NDVI INDUCED BY DIFFERENCES IN SPATIAL RESOLUTION UNDER A MULTIPLE-ENDMEMBER LINEAR MIXTURE MODEL

Kenta Obata[a] and Hiroki Yoshioka[a]

[a]Department of Information Science and Technology, Aichi Prefectural University
1522-3 Kumabari, Nagakute, Aichi, Japan
kenta.obata@cis.aichi-pu.ac.jp, yoshioka@ist.aichi-pu.ac.jp
Corresponding author's E-mail: yoshioka@ist.aichi-pu.ac.jp

KEY WORDS: Scaling Effect, NDVI, Error Bounds, Multiple-Endmember, Two-Endmember, Linear Mixture Model, Monotonicity

ABSTRACT:

Scaling effect of area-averaged NDVI is known as a source of error induced by differences in spatial resolution of two independent measurements over a fixed area. It deteriorates accuracy in parameter retrieval via NDVI, thus its mechanism needs to be fully understood for a better rectification of NDVI. The objective of this study is to investigate error bounds of averaged NDVI within a fixed area as a function of spatial resolution under assumptions of multiple-endmember linear mixture model (LMM). The NDVI behavior was first analyzed to identify the conditions regarding the choice of endmember spectra at which the averaged NDVI becomes the maximum and minimum. A series of numerical simulations were conducted by assuming a four-endmember LMM to demonstrate the finding such that the values of NDVI which show non-monotonic behavior fall into the ranges estimated from the two-endmember cases at all the resolutions by choosing appropriate pairs of endmember spectra predicted from the analysis. It was concluded that the error in the averaged NDVI over a fixed size of area composed of multiple endmembers can be bounded from the simpler two-endmember cases which would be a key to predicting the maximum and minimum errors caused by the scaling effect.

1 INTRODUCTION

Long-term monitoring of global vegetation status plays an important role to understand land-atmosphere interactions and their effects on climate change (Bounoua et al., 2000). To improve accuracy in climate change prediction, integration of the results from multiple sensors are needed (Los et al., 2000). However, differences in sensor specifications such as spatial resolution and spectral configuration could induce biases on parameter retrieval from remotely sensed satellite data (Price, 1999, Tucker et al., 2005, Pottier et al., 2006). For better interpretation of earth observation data, those errors need to be minimized based on a prior and posterior knowledge about sensor characteristics.

The scaling effect is a fundamental issue of remote sensing that induces biases in parameter retrieval over a fixed size of area among measurements with different spatial resolutions (Hu and Islam, 1997, Jiang et al., 2006). The scaling effect can be categorized into three (Chen, 1999), 1) effect of sampling schemes (or point spread function) (Settle, 2005), 2) nonlinear effect of retrieval algorithms (Hu and Islam, 1997, Jiang et al., 2006), and 3) effect of target heterogeneity (Hall et al., 1992, Friedl et al., 1995). This study focuses on the nonlinearity of spectral vegetation index as an example. This issue has been widely discussed up to date, yet, the uncertainty caused by the scaling effect has not been fully clarified.

Normalized difference vegetation index (NDVI) is a ratio of the difference between NIR and red band divided by their sum (Tucker, 1979). When the land surface is heterogeneous, an area-averaged NDVI shows biases caused by its nonlinearity of the model equation. Numerous studies have discussed its scaling effect. For example, those studies cover the themes of empirical investigations (Wood and Lakshmi, 1993, Cola, 1997), regression analysis (Aman et al., 1992, Maselli et al., 1998, Thenkabail, 2004), numerical experiments (Huete et al., 2005), and analytical studies (Hall et al., 1992, Hu and Islam, 1997, Jiang et al., 2006).

There are basically two approaches to this problem. The first approach is relative calibration of the outputs from two different sensors. In this approach, measurements from multiple sensors of different spatial resolutions are transformed into a common resolution by performing spatial averaging (Aman et al., 1992, Maselli et al., 1998, Thenkabail, 2004). Then, regression analysis is conducted to find a relationship among the sensors. This approach requires overlapping periods of data acquisition between the two datasets, which is the major drawback of this approach. The second approach is absolute calibration against the invariant values which are determined hypothetically under a specific condition. In this approach, the retrieved parameters from each pixel in any resolutions are transformed into the absolute values of an hypothetical case, for example, a case of extremely fine resolution at which all the pixels consist of only one class of surface (hence homogeneous). As a result, the VI value under the extreme case is invariant against variations of pixel scale (Hu and Islam, 1997). However, obtaining such an invariant value is a major challenge (obtaining the value itself is often a goal of retrieval algorithms).

To proceed the analysis one step further for the scaling issue, we try to predict the upper and lower limits of the error caused by the resolution differences. If it is possible to predict the error bounds of the NDVI caused by the scaling effects at any resolution case, it becomes easier to discriminate variations in NDVI caused by an environmental change from the one caused by the scaling effects. In addition, if the error bounds estimations can be performed at any resolution independently from the results at another resolution, the calibration technique does not require an overlapping period between the two datasets.

A key to this approach is monotonic behavior of averaged NDVI as a function of spatial resolution (represented by the number of pixel in this study.) In general, NDVI is not monotonic along with resolution. In our previous work, we found that there are certain sequences of resolutions in which the values of NDVI changes monotonically as resolution becomes finner under the assumptions of two-endmember linear mixture model (Yoshioka

et al., 2008). However, when the number of endmember spectra becomes larger than two, the value of NDVI is no longer monotonic. In this study, we investigate the error bounds of NDVI as a function of spatial resolution under multiple endmember assumptions.

2 BACKGROUND

2.1 Source of Scaling Effect on NDVI

An area averaged value of NDVI can be obtained by two steps. The first one is the band rationing process (retrieval algorithm) represented by a function f,

$$f(\boldsymbol{p}) = \frac{p_n - p_r}{p_n + p_r} \tag{1}$$

where $\boldsymbol{p} = (p_r, p_n)$ represents a measured spectrum. The subscripts r and n denote red and NIR bands, respectively. The second step is the spatial averaging process (spatial filtering) represented by a function g as the follow.

$$g(P) = \frac{1}{N}\sum_{k=1}^{N} P_k \tag{2}$$

where P represents observed values (either spectral reflectance or NDVI in this study), and the subscript k denotes an individual pixel. The integer N represents the number of pixel within a region of interest to be averaged over. Then, a source of the scaling effect on NDVI can be explained as a difference in the order of performing these two steps.

The algorithm called 'distributed case' (Hu and Islam, 1997), V_D, performs the index calculation prior to the spatial averaging process written as

$$V_D = (g \circ f)(\boldsymbol{p}). \tag{3}$$

On contrary, the algorithm called 'lumped case' (Hu and Islam, 1997), V_L, performs spatial averaging process first,

$$V_L = (f \circ g)(\boldsymbol{p}). \tag{4}$$

The output of the distributed case does not become identical to that of the lumped case because of surface heterogeneity and nonlinear of the function f.

$$V_D \neq V_L. \tag{5}$$

2.2 Scaling Effect on Area-Averaged NDVI Under the Assumption of Two-Endmember Linear Mixture Model

A value of NDVI averaged over a certain area changes as the spatial resolution of measurements (pixel size) changes. In general, the averaged value of NDVI changes non-monotonously along with spatial resolution. In order to predict an NDVI value at a certain resolution based on a result of relatively coarser resolution case, one needs to know a degree of uncertainty caused by the characteristic of non-monotonic behavior. For example, it seems to be impossible to estimate the maximum and minimum values of averaged NDVI as well as to identify the case of spatial resolutions at which the maximum and minimum occur. The variation range of NDVI value caused by the differences in spatial resolution is unpredictable without knowing the maximum and minimum values of NDVI as a function of spatial resolution. To predict the error bounds, area-averaged NDVI as a function of spatial resolution must be investigated thoroughly. If the averaged NDVI changes monotonously along with a certain resolution sequence, the NDVI values at the extreme resolutions certainly become the maximum or minimum. It also means that the averaged NDVI at intermediate resolutions do not exceed these extreme values. For this purpose, monotonicity of averaged NDVI along with the spatial resolution becomes a key to the identification of the error bounds.

Several studies have shed the light on monotonic behavior of area-averaged NDVI along with spatial resolution implicitly or explicitly (Hu and Islam, 1997, Jiang et al., 2006). In those studies, land surface is assumed to be composed of only two surface classes, vegetation and non-vegetation. Jiang et al. suggested that area-averaged NDVI would change monotonously from coarser to finer resolution (from lumped to distributed case), because the land surface heterogeneity within pixels would decrease as spatial resolution becomes higher (Jiang et al., 2006). Somewhat controversial conclusion is inferred from findings by several studies. For example, Hu et al. approximated the difference of area-averaged NDVI between the two cases of extreme resolution by a polynomial with variance and covariance of reflectance as its parameter (Hu and Islam, 1997). Based on their findings, area-averaged NDVI would not necessary be monotonic because variance and covariance of reflectance are not always varied monotonously from coarser to finer resolution.

Yoshioka et al. demonstrated that area-averaged NDVI changes monotonously as a function of spatial resolution within a certain resolution sequence based on a two-endmember linear mixture model (Yoshioka et al., 2008). With a resolution transfer model, difference of area-averaged NDVI between resolution level 1 and 2 (resolution level is the number of pixel within a fixed area.) are investigated analytically. From their findings, one could be clarified that magnitude relationship of averaged NDVI between resolution level j and $j+1$, $\overline{V}_j$ and $\overline{V}_{j+1}$ depends only on endmember spectrum of vegetation and non-vegetation for a fixed area, $\boldsymbol{\rho}_1$ and $\boldsymbol{\rho}_2$ (subscript, 1 and 2 represent vegetation and non-vegetation class, respectively) as follows,

$$\overline{V}_j \begin{cases} < \overline{V}_{j+1} & \text{when} \quad \eta < 1 \\ = \overline{V}_{j+1} & \text{when} \quad \eta = 1 \\ > \overline{V}_{j+1} & \text{when} \quad \eta > 1, \end{cases} \tag{6}$$

where

$$\eta = \frac{||\boldsymbol{\rho}_1||}{||\boldsymbol{\rho}_2||}. \tag{7}$$

Equation (6) implies that an averaged NDVI varies monotonically as a function of spatial resolution within resolution sequences obtained by the resolution transfer model (forward and backward use of partitioning rule (Yoshioka et al., 2008)). Therefore, averaged NDVI at extreme resolution, $\overline{V}_1$ and $\overline{V}_\infty$ becomes maximum and minimum because 1) averaged NDVI changes monotonous from coarser to finer resolution within a certain resolution sequence and 2) extreme resolution can be yielded by forward and reverse use of partitioning rule. Thus error bounds of scaling effect could be specified by these values within two-endmember assumption.

2.3 Example of Scaling Effect Under Three-endmember Linear Mixture Model

Area-averaged NDVI does not show monotonic behavior under the three-endmember linear mixture model. We will provide one such example in this subsection. Figure 1 shows a hypothetical field composed of three classes of surface (hence three endmembers), i.e., one vegetation class and two soil classes (soil-1 and soil-2). Spectral reflectances of red and NIR band of the

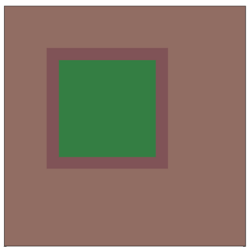

Figure 1: Hypothetical field with three endmembers which are vegetation and two types of soil surfaces (dark soil and bright soil). Red and NIR reflectances for the vegetation endmember are 0.05 and 0.4, respectively. The spectra of the dark soil and bright soil are $(0.15, 0.15)$ and $(0.25, 0.25)$, respectively.

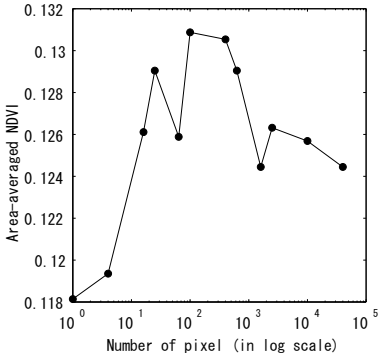

Figure 2: Area-averaged NDVI with three-endmember linear mixture model as a function of spatial resolution.

three endmembers are $(0.05, 0.4)$, $(0.15, 0.15)$, and $(0.25, 0.25)$ for the vegetation, soil-1 and soil-2 classes, respectively. Area-averaged values of NDVI for this field were obtained by assuming several resolutions (Fig. 1). Figure 2 is the plot of averaged NDVI as a function of spatial resolution. In the figure, the maximum appears at an intermediate resolution, which clearly indicates the fact that the range of NDVI variation cannot be estimated by the two extreme resolution cases (coarsest and finest resolution cases).

Since the maximum and/or minimum value may occur at intermediate resolution case, the approach taken for the two-endmember case cannot be applicable in the three-endmember (and higher) cases. The purpose of this study is to demonstrate a key characteristics of NDVI behavior as a function of spatial resolution under multiple-endmember LMM.

3 SCALING EFFECT ON AREA-AVERAGED NDVI WITH MULTIPLE ENDMEMBER LINEAR MIXTURE MODEL

The maximum and minimum values of NDVI at a resolution case can be estimated by finding the maximum and minimum value NDVI for each pixel at any resolution cases. Thus, we need to find the maximum and minimum bounds of the area averaged NDVI for a given single pixel which contains three (or more) types of surfaces (endmembers). For this purpose, we took an approach to find the minimum and maximum values of NDVI as a function of endmember spectra under a fixed value of fraction of vegetation cover.

3.1 Assumptions and Definitions

We divide the endmember classes into two categories which are vegetation and non-vegetation. We then assume that the endmember spectra of vegetation classes fall into a single NDVI isoline as illustrated in Fig. 3 so that the differences in spectra are simply the magnitude of the reflectance (or brightness). Likewise, the spectra of the non-vegetation endmembers fall into a single soil line. In this study, we assumed that the soil line is identical to one of the NDVI isolines whose NDVI value is zero (also illustrated in Fig. 3.)

We focus on a behavior of NDVI within a single pixel, represented by V_1 (resolution level $j = 1$), as a function of endmember spectra under a fixed value of vegetation fraction. The average reflectance spectrum of each category can be written as a wighted sum of all the i-th endmembers $\boldsymbol{\rho}_{iq}$ (either vegetation ($i = 1$) or non-vegetation ($i = 2$)) using ω_{iq} as weights for $\boldsymbol{\rho}_{iq}$. Subscript q represents the individual endmember for the i-th category. Then we have

$$\overline{\boldsymbol{\rho}}_i = (\overline{\rho}_{ri}, \overline{\rho}_{ni}) = \frac{1}{\Omega_i} \sum_{q=1}^{M_i} \omega_{iq} \boldsymbol{\rho}_{iq}, \tag{8}$$

where $\overline{\rho}_{ri}$ and $\overline{\rho}_{ni}$ are red and NIR reflectances of the i-th endmember category, respectively. M_i represents the number of endmember for the i-th category. Ω_i is defined as

$$\Omega_i = \sum_{q=1}^{M_i} \omega_{iq}. \tag{9}$$

The reflectance spectrum under the multipel-endmember assumption $\boldsymbol{\rho}_m = (\rho_{mr}, \rho_{mn})$ can be represented by weighted average of endmember spectra for vegetation and non-vegetation categories, $\overline{\boldsymbol{\rho}}_1$ and $\overline{\boldsymbol{\rho}}_2$, respectively.

$$\boldsymbol{\rho}_m = \Omega_1 \overline{\boldsymbol{\rho}}_1 + (1 - \Omega_1) \overline{\boldsymbol{\rho}}_2. \tag{10}$$

Since we assume that the reflectance spectra of each endmebmer are aligned in a single NDVI isoline, both $\overline{\boldsymbol{\rho}}_1$ and $\overline{\boldsymbol{\rho}}_2$ change along with the NDVI isolines illustrated as a green and a brown dashed line in Fig. 3.

Using these assumptions and definitions, V_1 under the multiple endmember case can also be written by the same form of the two-endmember case as,

$$V_1 = \frac{\rho_{mn} - \rho_{mr}}{\rho_{mn} + \rho_{mr}} \tag{11}$$

$$= \frac{\Omega_1(\alpha - 1)\overline{\rho}_{r1} + (1 - \Omega_1)(\overline{\rho}_{n2} - \overline{\rho}_{r2})}{\Omega_1(\alpha + 1)\overline{\rho}_{r1} + (1 - \Omega_1)(\overline{\rho}_{n2} + \overline{\rho}_{r2})} \tag{12}$$

where α represents the slope of the NDVI isoline for vegetation class,

$$\alpha = \frac{\overline{\rho}_{n1}}{\overline{\rho}_{r1}}. \tag{13}$$

3.2 V_1 as a Function of η

Partial derivative of V_1 with respect to $\overline{\rho}_{r1}$ becomes

$$\frac{\partial V_1}{\partial \overline{\rho}_{r1}} = \frac{2\Omega(1 - \Omega)(\alpha\overline{\rho}_{r2} - \overline{\rho}_{n2})}{[\Omega(1 + \alpha)\overline{\rho}_{r1} + (1 - \Omega)(\overline{\rho}_{n2} - \overline{\rho}_{r2})]^2}. \tag{14}$$

In this equation, the term, $(\alpha\overline{\rho}_{n2} - \overline{\rho}_{r2})$ becomes positive, because the NDVI value of the vegetation category is larger than

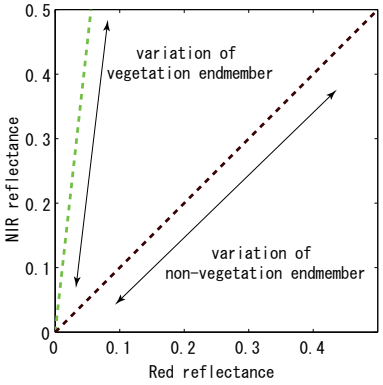

Figure 3: Illustration about variation of vegetation and non-vegetation spectrum within a multiple-endmember LMM assumed in this study.

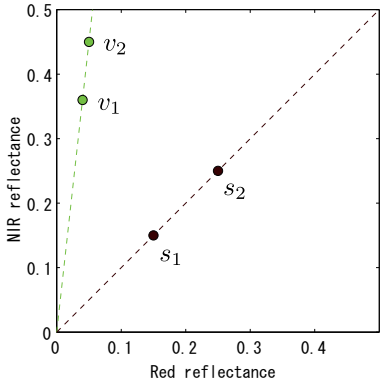

Figure 4: Endmember spectra for vegetation and non-vegetation surfaces in red-NIR reflectance space. Differences in the endmember spectra among the classes are 1-norm which represents magnitude of the spectra (brightness). v_1 and v_2 denote vegetation endmembers, and s_1 and s_2 denote non-vegetation endmembers.

that of the non-vegetation category.

$$\frac{\overline{\rho}_{n1}}{\overline{\rho}_{r1}} - \frac{\overline{\rho}_{n2}}{\overline{\rho}_{r2}} > 0. \tag{15}$$

Thus, all the terms in $\frac{\partial V_1}{\partial \overline{\rho}_{r1}}$ become positive, which leads to the fact that $\frac{\partial V_1}{\partial \overline{\rho}_{r1}}$ is always positive. It means that V_1 increases monotonically as a function of $\overline{\rho}_{r1}$. Finally, since η increases monotonically as a function of $\overline{\rho}_{r1}$, V_1 also increases monotonically with η.

3.3 Error Bounds of Averaged NDVI as a Function of Endmember Spectra

In the previous subsection it was shown that V_1 changes monotonically as a function of $\overline{\rho}_{r1}$. It implies that V_1 becomes the maximum ($V_{1,max}$) when

$$\overline{\rho}_{r1} = \rho_{r,max} = max\{\rho_{r,1q}\}, \ \ (1 \le q \le M_1), \tag{16}$$

$$V_{1,max} = \frac{\Omega_1(\alpha-1)\rho_{r,max} + (1-\Omega_1)(\overline{\rho}_{n2} - \overline{\rho}_{r2})}{\Omega_1(\alpha+1)\rho_{r,max} + (1-\Omega_1)(\overline{\rho}_{n2} + \overline{\rho}_{r2})}. \tag{17}$$

Likewise, V_1 becomes minimum ($V_{1,min}$) when

$$\overline{\rho}_{r1} = \rho_{r,min} = min\{\rho_{r,1q}\}, \ \ (1 \le q \le M_1), \tag{18}$$

$$V_{1,min} = \frac{\Omega_1(\alpha-1)\rho_{r,min} + (1-\Omega_1)(\overline{\rho}_{n2} - \overline{\rho}_{r2})}{\Omega_1(\alpha+1)\rho_{r,min} + (1-\Omega_1)(\overline{\rho}_{n2} + \overline{\rho}_{r2})}. \tag{19}$$

The value of V_1 can be bounded by the choice of the two extreme endmembers ($\rho_{r,max}$ and $\rho_{r,min}$.) The similar results can be obtained about the endmember choice of the non-vegetation category. In summary, the error bounds of V_1 for the case of multiple endmembers can be estimated by the choice of these extreme choices about the endmember spectra under the assumptions we made in this study. These findings infer the followings: Although the area averaged NDVI $\overline{V}_j$ does not show monotonic behavior (hence the maximum and/or minimum may occurs at an intermediate resolution), V_1 falls within the range between $V_{1,max}$ and $V_{1,min}$. We will examine this implication in the next section by conducting a numerical experiment.

4 NUMERICAL VALIDATION

4.1 Scaling Effect on NDVI as a Function of η

Numerical experiments were conducted to validate error bounds of scaling effect on averaged NDVI under multiple endmember

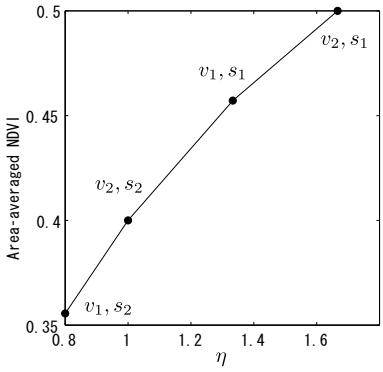

Figure 5: Area-averaged NDVI as a function of η.

cases derived in this study. First, the dependency of the scaling effect on the parameter η was examined assuming various resolution cases for a fixed value of vegetation cover.

The hypothetical field consists of two vegetation and two soil endmembers (total of four endmembers) shown in Fig. 4. The reflectance spectra of the two vegetation endmembers were chosen from an identical NDVI isoline resulting the same NDVI value for the pure signals. Thus, the only difference between the two spectra is the brightness (magnitude). It leads to a difference in the value of η depending on the choice of the spectrum. Similarly, the endmemer spectra for the non-vegetation surfaces were chosen from the soil line of which the slope and offsets are 1.0 and 0.0, respectively. This soil line is identical to the NDVI isoline whose VI value is zero (Fig. 4). The four endmember spectra represented by v_1, v_2, s_1 and s_2 in Fig. 4 are set as follows: $v_1 = (0.04, 0.36)$, $v_2 = (0.05, 0.45)$, $s_1 = (0.15, 0.15)$, and $s_2 = (0.25, 0.25)$.

To demonstrate the variations of NDVI as a function of η, we prepared a set of mixed signals under 50% of vegetation cover for all the four combinations of vegetation and non-vegetation endmember spectra. The computed NDVI values (V_1) are plotted as a function of η in Fig. 5. From the figure, V_1 depends on η, and increases monotonically along with η as expected from the previous section. These results also imply that the VI values of multiple endmember with those four spectra fall into the range of two extreme combinations, namely, the choice of v_1 and s_2 for

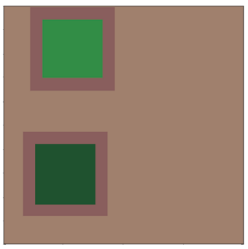

Figure 6: Hypothetical field with four endmembers including two types of vegetation and two types on non-vegetation classes. The red and NIR reflectances for each endmember are the same values assumed in Fig.5.

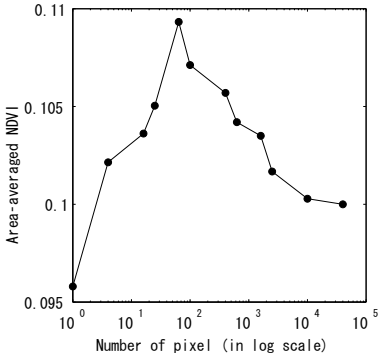

Figure 7: Area-averaged NDVI as a function of spatial resolution with a four-endmember linear mixture model.

the minimum bound and the choice of v_2 and s_1 for the maximum bound.

4.2 Error Bounds of NDVI as a Function of Spatial Resolution

The next example is about the four endmember cases. We will demonstrate how the non-monotonic variations of NDVI can be bounded by the two endmember cases by choosing vegetation and non-vegetation spectra appropriately. A hypothetical field was also assumed (illustrated in Fig. 6) which consists of all the four spectra assumed in the previous subsection (also plotted in Fig. 4).

The areas represented by the dark and light green patches in Fig. 6 denote the surfaces covered by v_1 and v_2, respectively. While, the areas represented by the dark and light brown patches denote the surfaces covered by s_1 and s_2. This hypothetical target were divided into pixels to simulate various resolutions to obtain the averaged NDVI as a function of spatial resolution which is represented by the number of pixel within the target area. Figure 7 shows the plot of NDVI along with the number of pixel included within the target area. The maximum value occurs at an intermediate resolution. The figure clearly shows non-monotonic behavior under the four endmember case. The error bounds cannot be estimated from the lowest and highest resolution cases, which is the major difference from the two endmember cases.

To demonstrate the error bounds induced by the variation in spatial resolution under the multiple endmember assumptions, the vegetation and non-vegetation endmembers are altered with the spectra which results in the highest and lowest value of η. After this alteration, we have two cases of two endmember assumptions illustrated in Figs. 8 and 9. Note that the fraction of vegetation

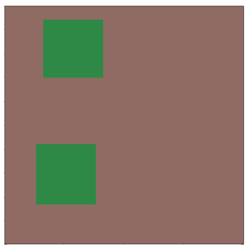

Figure 8: Altering image with brighter vegetation and darker soil which maximize the value of η.

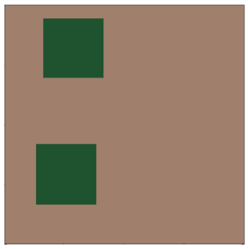

Figure 9: Altering image with darker vegetation and brighter soil which minimize the value of η.

cover remains the same for all the cases shown in Figs. 6, 8, and 9. The averaged NDVI for the two endmember cases (Figs. 8, and 9) are plotted with the original problem in Fig. 10. In the figure, the black solid line represents the NDVI of the original case (with the four endmembers), and the blue and red dashed lines represent the NDVI of the altering cases (two endmember cases) of Figs. 8 and 9, respectively. The figure clearly shows that the NDVI of the original four endmember cases falls into the values between the two of the two endmember cases, which is also expected from the analysis of the previous section. Although $\overline{V}_\infty$ is between $V_{1,min}$ and $V_{1,max}$ in this example, $\overline{V}_\infty$ would exceed this range. Such an example can be easily imagine, e.g., to consider a case in which both two endmember cases (red and blue dashed lines) becomes increasing trend simultaneously. In such a case, $\overline{V}_\infty$ becomes larger than $V_{1,max}$, thus it becomes the maximum bound. Therefore, these results imply that the error bounds can be estimated from the three values, namely, 1) $V_{1,max}$, 2) $V_{1,min}$, and 3) $\overline{V}_\infty$.

5 DISCUSSION AND CONCLUSIONS

The scaling effect of NDVI had been investigated under the assumptions of four-endmember LMM. The influence of endmember spectra was discussed analytically to find the condition under which two-endmember (instead of four-endmember) cases of identical vegetation cover result in the maximum and minimum values among the cases of two endmember choices. From the findings of our previous work about the monotonicity of NDVI under the two-endmember LMM, we found that the error bounds of the NDVI induced by the scaling effect under the assumptions of multiple-endmember LMM can be bounded by the values of the three extreme resolution cases ($V_{1,min}$, $V_{1,max}$, and $\overline{V}_\infty$) of two-endmember LMM with appropriate choices of endmember spectra.

A set of numerical experiments were then conducted to validate the findings. Although the experiments clearly justify our theoretical findings, those experiments would never be enough to

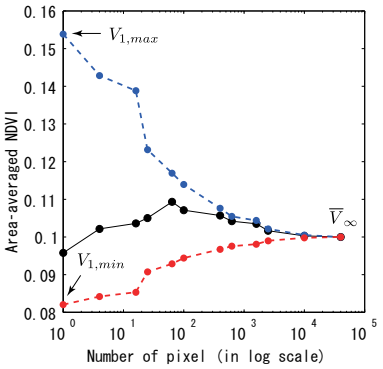

Figure 10: Area averaged NDVI as a function of spatial resolution for the hypothetical fields shown in Fig.6, 8, and 9. Averaged NDVI for the original image (Fig.6) is within a range defined by the two altering images (Fig.8 and 9).

validate our theory. Further comprehensive experiments would be needed to fully validate the theory. Moreover, applications of the findings to actual data processing of satellite images will be needed with the invention of error estimation technique based on the theory.

To extend this study to practical use, $\overline{V}_{1,min}$, $\overline{V}_{1,max}$, and $\overline{V}_{\infty}$ must be estimated from a measured spectrum of the target pixel. In addition, the two endmember spectra must be obtained within a reasonable accuracy. Although there are techniques to extract the averaged endmember spectra (Obata et al., 2008), those estimation/extraction would be a major source of difficulties in the application of the theoretical findings.

Finally, the scaling effects are not limited to NDVI. Other spectral vegetation indices such as SAVI and EVI and the parameter retrieval algorithms using band ratios would also suffer from the scaling effects. The influences of the scaling effects on those algorithms needs to be invested from both the theoretical and practical view points.

REFERENCES

Aman, A., Randriamanantena, H. P., Podaire, A. and Frouin, R., 1992. Upscale integration of normalized difference vegetation index: the problem of spatial heterogeneity. IEEE Trans. Geosci. Remote Sens. 30(2), pp. 326–338.

Bounoua, L., Collatz, G. J., Los, S. O., Sellers, P. J., Dazlich, D. A., Tucker, C. J. and Randall, D. A., 2000. Sensitivity of climate to changes in NDVI. J. Climate 13(13), pp. 2277–2292.

Chen, J., 1999. Spatial scaling of a remotely sensed surface parameter by contexture. Remote Sens. Environ. 69, pp. 30–42.

Cola, L. D., 1997. Multiresolution covariation among Landsat and AVHRR vegetation indices. In: D. A. Quattrochi and M. F. Goodchild (eds), Scale in Remote Sensing and GIS, Boca Raton, Florida: Lewis, pp. 73–91.

Friedl, M. A., Davis, F. W., Michaelsen, J. and Moritz, M. A., 1995. Scaling and uncertainty in the relationship between the NDVI and land surface biophysical variables: an analysis using a scene simulation model and data from FIFE. Remote Sens. Environ. 54, pp. 233–246.

Hall, F. G., Huemmrich, K. F., Goetz, S. J., Sellers, P. J. and Nickeson, J. E., 1992. Satellite remote sensing of surface energy balance: success, failures, and unresolved issues in FIFE. J. Geophys. Res. 97(D17), pp. 19,061–19,089.

Hu, Z. and Islam, S., 1997. A frame work for analyzing and designing scale invariant remote sensing algorithms. IEEE Trans. Geosci. Remote Sens. 35(3), pp. 747–755.

Huete, A., Kim, H.-J. and Miura, T., 2005. Scaling dependencies and uncertainties in vegetation index - biophysical retrievals in heterogeneous environments. In: IEEE IGARSS05, Vol. 7, pp. 5029–5032.

Jiang, Z., Huete, A. R., Chen, J., Chen, Y., Yan, G. and Zhang, X., 2006. Analysis of ndvi and scaled difference vegetation index retrievals of vegetation fraction. Remote Sens. Environ. 101, pp. 366–378.

Los, S. O., Pollack, N. H., Parris, M. T., Collatz, G. J., Tucker, C. J., Sellers, P. J., Malmstrom, C. M., DeFries, R. S., Bounoua, L. and Dazlich, D. A., 2000. A global 9-yr biophysical land surface dataset from NOAA AVHRR data. J. Hydrometeorol. 1(2), pp. 183–199.

Maselli, F., Gilabert, M. A. and Conse, C., 1998. Integration of high and low resolution NDVI data for monitoring vegetation in Mediterranean environments. Remote Sens. Environ. 63, pp. 208–218.

Obata, K., Yoshioka, H. and Yamamoto, H., 2008. Unmixing a variable endmember linear mixture model for estimation of heat island mitigation by green vegetation. In: IEEE IGARSS08, Vol. 5, pp. 498–501.

Pottier, C., Garcon, V., Larnicol, G., Sudre, G., Schaeffer, P. and Traon, P.-Y. L., 2006. Merging SeaWIFS and MODIS/Aqua ocean color data in North and Equatorial Atlantic using weighted averaging and objective analysis. IEEE Trans. Geosci. Remote Sens. 44(11), pp. 3436–3451.

Price, J. C., 1999. Combining multispectral data of differing spatial resolution. IEEE Trans. Geosci. Remote Sens. 37(3), pp. 1199–1203.

Settle, J. J., 2005. On the residual term in the linear mixture model and its dependence on the point spread function. IEEE Trans. Geosci. Remote Sens. 43(2), pp. 398–401.

Thenkabail, P. S., 2004. Inter-sensor relationships between IKONOS and Landsat-7 ETM+ NDVI data in three ecoregions of Africa. Int. J. Remote Sens. 20(2), pp. 389–408.

Tucker, C. J., 1979. Red and photographic infrared linear combinations for monitoring vegetation. Remote Sens. Environ. 8, pp. 127–150.

Tucker, C. J., Pinzon, J. E., Brown, M. E., Slayback, D. A., Pak, E. W., Mahoney, R., Vermote, E. F. and Saleous, N. E., 2005. An extended AVHRR 8-km NDVI dataset compatible with MODIS and SPOT vegetation NDVI data. Int. J. Remote Sens. 26(20), pp. 4485–4498.

Wood, E. F. and Lakshmi, V., 1993. Scaling water and energy fluxes in climate systems: three land-atmospheric modeling experiments. J. Climate 6(5), pp. 839–857.

Yoshioka, H., Wada, T., Obata, K. and Miura, T., 2008. Monotonicity of area averaged NDVI as a function of spatial resolution based on a variable endmember linear mixture model. In: IEEE IGARSS08, Vol. 3, pp. 415–418.